Theoretical transition dipole moments and lifetimes for the $A\,^1\Sigma_u^+ \rightarrow X\,^1\Sigma_g^+$ system of Na_2*

W. J. Stevens and M. M. Hessel

Laser Physics Section, National Bureau of Standards, Boulder, Colorado 80302

P.J. Bertoncini and A.C. Wahl

Argonne National Laboratory, Argonne, Illinois 60439
(Received 22 July 1976)

Multiconfiguration self-consistent field (MCSCF) calculations have been carried out on the $X\,^1\Sigma_g^+$, $A\,^1\Sigma_u^+$, and $B\,^1\Pi_u$ states of Na_2. The calculated potential energy curves are in good agreement with the experimental X and A RKR curves of Hessel and Kusch. Both the $A \rightarrow X$ and $B \rightarrow X$ transition moments have been calculated as a function of nuclear separation using MCSCF wavefunctions. These calculations are in excellent agreement with the recent experimental determinations of the $B \rightarrow X$ transition moment. A values and lifetimes of several A-state vibrational and rotational levels for the $A \rightarrow X$ transition have been calculated using the theoretical transition moment and the experimental potential curves of Hessel and Kusch. These again are in excellent agreement with the recently measured lifetimes.

I. INTRODUCTION

The $A\,^1\Sigma_u^+ \rightarrow X\,^1\Sigma_g^+$ system of Na_2 has recently drawn interest as a possible visible wavelength laser candidate.[1] Several features of the A state of Na_2 make it a desirable laser species. The $A\,^1\Sigma_u^+$ equilibrium nuclear separation is larger than that of the X state, which results in an emission spectrum with maximum intensity shifted to the red of the absorption maximum. This fact makes inversion relatively easy to achieve, since the lowest vibrational levels of the A state radiate preferentially to higher, relatively unpopulated levels of the ground state. The ^2P excited state of Na, which gives rise to the $A\,^1\Sigma_u^+$ molecular state via recombination with ground state atoms, can be populated readily in a discharge because of the large $ns \rightarrow np$ electron excitation cross section for the alkali resonance line. The modeling of the Na_2 laser is, however, complicated by possible nonradiative deactivation of the A state by curve crossings with other molecular states.

The spectroscopy of the low-lying singlet states of Na_2 is well understood. Hessel and Kusch[2] have recently completed accurate analyses of the $X\,^1\Sigma_g^+$, $A\,^1\Sigma_u^+$, and $B\,^1\Pi_u$ states from high resolution laser fluorescence and absorption spectra. They have also observed[3] and analyzed[4] perturbations in the $A\,^1\Sigma_u^+$ state due to curve crossings with the $a\,^3\Pi_u$ state. The radiative lifetimes of the excited singlets (which are important parameters in laser modeling) have also been studied. Reliable data, including transition dipole moments, for the $B\,^1\Pi_u$ state are available from Hessel *et al.*[5] and more recently from Demtröder *et al.*[6] Lifetime measurements for $A\,^1\Sigma_u^+$ have recently become available. Kleppner[7] has measured the lifetimes of several vibrational levels by a molecular beam, laser-induced fluorescence technique, but these measurements do not include resolution of individual rotational levels, nor do they provide absolute probabilities for individual transitions.

With an accurate knowledge of the potential energy curves and the transition dipole moment as a function of nuclear separation, it is a straightforward task to calculate the absolute transition probabilities for molecular v, J transitions. In this paper, we have combined the RKR curves of Hessel and Kusch[2] with an accurate *ab initio* theoretical determination of the Na_2 $A\,^1\Sigma_u^+ - X\,^1\Sigma_g^+$ transition dipole moment in order to calculate the radiative transition probabilities for the $A\,^1\Sigma_u^+$ state.

II. *AB INITIO* CALCULATIONS

A. Multiconfiguration self-consistent-field (MCSCF) method

The energies of the low-lying excited states of Na_2 have been studied previously by Bertoncini and Wahl.[8] Our efforts here essentially duplicate their work for the singlet states, with particular attention being paid to optimization of the wavefunctions. Electronic properties such as the transition dipole moment are much more sensitive to wavefunction optimization than are electronic energies. To solve the electronic Schrödinger equation, we have used the multiconfiguration self-consistent-field method (MCSCF) as developed by Das and Wahl.[9] Since the details of this method have been discussed elsewhere, we will give only a brief summary here.

We start with the electronic Schrödinger equation in the Born–Oppenheimer approximation

$$H(\mathbf{r}_1, \mathbf{r}_2, \cdots, \mathbf{r}_n, \mathbf{R}_1, \mathbf{R}_2, \cdots, \mathbf{R}_N)\,\Psi(\mathbf{r}_1, \mathbf{r}_2, \cdots, \mathbf{r}_n) = E(\mathbf{R}_1, \mathbf{R}_2, \cdots, \mathbf{R}_N)\,\Psi(\mathbf{r}_1, \mathbf{r}_2, \cdots, \mathbf{r}_n), \tag{II. 1}$$

where $\mathbf{r}_n$ is the position vector of electron n and $\mathbf{R}_N$ is the position vector of nucleus N (held fixed while solving for Ψ). H is the usual spinfree Hamiltonian given in atomic units by

$$H(\mathbf{r}_1, \mathbf{r}_2, \cdots, \mathbf{r}_n, \mathbf{R}_1, \mathbf{R}_2, \cdots, \mathbf{R}_N) = -\sum_i \frac{1}{2}\nabla_i^2 + \sum_a \frac{Z_a}{|\mathbf{r}_i - \mathbf{R}_a|} + \sum_{i<j}\sum \frac{1}{|\mathbf{r}_i - \mathbf{r}_j|} + \frac{Z_a Z_b}{|\mathbf{R}_a - \mathbf{R}_b|}. \tag{II. 2}$$

In the MCSCF method, the wavefunction Ψ is expanded as a configuration interaction (CI) series

$$\Psi(\mathbf{r}_1, \mathbf{r}_2, \cdots, \mathbf{r}_n) = \sum_K A_K \Phi_K(\mathbf{r}_1, \mathbf{r}_2, \cdots, \mathbf{r}_n). \quad \text{(II. 3)}$$

The configurations Φ are properly projected linear combinations of Slater determinants over a set of molecular orbitals ϕ:

$$\Phi_K(\mathbf{r}_1, \mathbf{r}_2, \cdots, \mathbf{r}_n) = \mathcal{O}_{L,S} \left| \phi_1(\mathbf{r}_1)\bar{\phi}_1(\mathbf{r}_2)\cdots\phi_q(\mathbf{r}_n) \right|. \quad \text{(II. 4)}$$

Here the symbol $\mathcal{O}_{L,S}$ is used to denote projection to an eigenfunction of angular momentum and spin. The electron spins are denoted by the presence or absence of a bar above the orbital, representing β or α spin functions, respectively. The space parts of the molecular orbitals ϕ are expanded in terms of some suitably chosen basis functions χ,

$$\phi_i = \sum_j c_{ij}\chi_j, \quad \text{(II. 5)}$$

with the restriction that $\int \phi_i \phi_j d\tau = \delta_{ij}$. The MCSCF procedure determines the CI mixing coefficients A_K and the molecular orbital expansion coefficients c_{ij} by variationally minimizing the energy in Eq. (II. 1).

The MCSCF method is ideally suited for calculating electronic properties as a function of nuclear separation, since the orbitals as well as the CI mixing coefficients are optimized for each geometry. With the proper choice of configurations, the orbital optimization guarantees a smooth description of the dissociation of the molecule into its constituent atoms in their proper states. The choice of configurations for the alkali dimers is discussed below in Sec. IIC.

B. The choice of basis set

A basis set of atomic-centered Slater-type orbitals (STO) was used for the Na_2 calculations. The STO's have the form

$$\chi_{NLM} = A_N r^{N-1} e^{-\xi r} Y_{LM}(\theta, \phi), \quad \text{(II. 6)}$$

TABLE I. STO basis set for Na_2.[a]

Symmetry block	Function	Exponent
Sigma	1*s*	10.159
	1*s*	15.333
	3*s*	6.257
	2*s*	2.977
	3*s*	0.862
	4*s*	0.929
	2*p*	4.176
	2*p*	7.719
	2*p*	2.275
	3*p*	1.200
	3*p*	0.800
	3*d*	0.8594
	3*d*	0.580
Pi	2*p*	4.176
	2*p*	7.719
	2*p*	2.275
	3*p*	1.200
	3*p*	0.800
	3*d*	0.8594
	3*d*	0.580

[a]The same set of functions was placed at each nuclear center.

where A_N is the normalization, ξ is the orbital exponent, and Y_{LM} is the usual spherical harmonic. This set was chosen to give an accurate representation of the Na atoms in the ^2S and ^2P states, and also to allow for distortion of the atomic orbitals in the chemical bonding region. For the ground state of the sodium atom a highly optimized basis was taken from the compilation of Bagus, Gilbert, and Roothaan.[10] Two 3*p* STO's were added to this basis and their exponents optimized to give the lowest energy for the ^2P atomic state. Two 3*d* STO's were also added for polarization effects in the bonding region. The 3*d* exponents were selected on the basis of Na_2 pseudopotential calculations by Bardsley *et al.*[11] The final basis set is given in Table I. Due to the size of the basis, the exponents were held fixed for all calculations. If the basis is sufficiently saturated, exponent optimization at each nuclear separation has only a minor effect. Using this basis, the Hartree–Fock energies for the ^2S and ^2P states of Na are -161.85745 and -161.78471 hartree, respectively. This gives a $^2S \rightarrow {}^2P$ excitation energy of 0.07274 hartree or 1.979 eV. The experimental excitation energy is 2.102 eV.

C. Results for the $X\,^1\Sigma_g^+$ state

Due to the fact that the atomic cores are highly localized and do not participate in the chemical bonding, only the two valence electrons need to be considered in the CI expansion. In each configuration, the core electrons are described by closed-shell orbitals which are optimized by the self-consistent-field part of the MCSCF. The core is denoted by $[\text{core}] = 1\sigma_g^2 1\sigma_u^2 2\sigma_g^2 2\sigma_u^2 3\sigma_g^2 3\sigma_u^2 1\pi_u^4 1\pi_g^4$. The core molecular orbitals are generally given by $1\sigma_g = 1/\sqrt{2}\,(1s_A + 1s_B)$, $1\sigma_u = 1/\sqrt{2}\,(1s_A - 1s_B)$, etc., although some distortion does occur at small nuclear separations.

The principle configuration for the $X\,^1\Sigma_g^+$ state at the equilibrium nuclear distance (R_e) is $[\text{core}]\,4\sigma_g^2$. However, an additional configuration $[\text{core}]\,4\sigma_u^2$ is needed to properly describe the dissociation of the molecule into two ^2S atoms. At large separations the two configurations have comparable mixing coefficients which become identical at $R=\infty$. The MCSCF guarantees that at infinite separation the $4\sigma_g$ and $4\sigma_u$ will become symmetric and antisymmetric linear combinations of the atomic 3*s* Hartree–Fock orbitals.

It can be shown[12] that for a two electron configuration expansion such as we have for the $X\,^1\Sigma_g^+$ state, only closed shell double excitations need to be considered if the orbitals are variationally optimized. All single excitations and open shell double excitations are included implicitly by the SCF optimization process. The resulting orbitals are the natural orbitals[12] of the two electron expansion. Our final wavefunction for the ground state of Na_2 includes eight configurations. In addition to the two "base" configurations discussed above, we have included $5\sigma_g^2$, $5\sigma_u^2$, $2\pi_u^2$, $2\pi_g^2$, $1\delta_u^2$, and $1\delta_g^2$. The most important of these are $5\sigma_g^2$ and $2\pi_u^2$. Table II shows the variation of the configuration mixing coefficients with nuclear separation, and the importance of the multiconfiguration expansion in describing the electronic distribution as a function of R.

TABLE II. Configuration mixing coefficients for the $X\,^1\Sigma_g^+$ state of Na_2.

Configuration \ R[a]	4.5	6.0	9.0	∞
[core] $4\sigma_g^2$	0.95385	0.95435	0.89775	0.70711
[core] $4\sigma_u^2$	−0.15277	−0.18237	−0.41236	−0.70711
[core] $5\sigma_g^2$	−0.01093	−0.09706	−0.09300	0.0
[core] $5\sigma_u^2$	−0.00209	−0.00846	−0.00405	0.0
[core] $2\pi_u^4$	−0.25779	−0.21476	−0.12360	0.0
[core] $2\pi_g^2$	−0.00456	−0.01476	−0.00563	0.0
[core] $1\delta_u^4$	−0.01513	−0.01049	−0.00489	0.0
[core] $1\delta_g^2$	−0.00131	−0.00413	−0.00222	0.0

[a]R = nuclear separation in bohrs. 1 bohr = 0.0529177 nm.

The energies for the $X\,^1\Sigma_g^+$ state are given in Table III and a plot of the calculated potential energy curve is shown in Fig. 1 along with the experimental RKR curve of Hessel and Kusch.[2] The small disagreements between theory and experiment for the X state are not of concern, since the experimental curves are used in the transition probability calculations.

D. Results for the $A\,^1\Sigma_u^+$ state

The $A\,^1\Sigma_u^+$ state arises from the $^2S+^2P$ atomic asymptote. It is described primarily by the configuration [core] $4\sigma_g 5\sigma_u$ at R_e. However, it is necessary, once again, to include a second configuration [core] $4\sigma_u 5\sigma_g$ to insure proper dissociation into ^2S and ^2P atoms. Asymptotically, $5\sigma_u$ and $5\sigma_g$ become $1/\sqrt{2}[3p\sigma_A - 3p\sigma_B]$, and $1/\sqrt{2}\,[3p\sigma_A + 3p\sigma_B]$, respectively. In addition to these two configurations we have also added $2\pi_u 2\pi_g$ and $1\delta_u 1\delta_g$. Table IV shows the importance of each of these configurations and the variation of the mixing coefficient with R.

At $R=\infty$ only the two base configurations contribute to the wavefunction. Formally, all molecular orbitals become symmetric or antisymmetric linear combinations of the appropriate atomic orbitals. By taking sums and differences of the *gerade* and *ungerade* molecular orbitals it is possible to rewrite the asymptotic wavefunction in localized form

$$\Psi_{R=\infty}(A\,^1\Sigma_u^+) = \tfrac{1}{2}A[[\text{core}]_A[\text{core}]_B\,3s_A(1)\,3p\sigma_B(2) + 3p\sigma_A(1)\,3s_B(2) + 3s_A(2)\,3p\sigma_B(1) + 3p\sigma_A(2)\,3s_B(1)]\Theta_{\text{spin}}. \quad \text{(II. 7)}$$

Here we have let A represent the antisymmetrizer and Θ_{spin} the singlet spin function. The valence electrons are numbered 1 and 2. A problem presents itself immediately when the wavefunction is written in this form. The ground and excited state atoms have the same core distribution. This is obviously not true in reality, and the calculational restriction leads to an asymptotic energy which is higher than the sum of the two atomic energies that were calculated individually and reported in Sec. II B. Comparing the computed asymptotic energy with the atomic energy sum, we find an error of 0.00643 hartree or 0.175 eV. We also expect a small error to be introduced in the transition moment at large R due to the core restrictions.

The theoretical potential energy curve plotted in Fig.

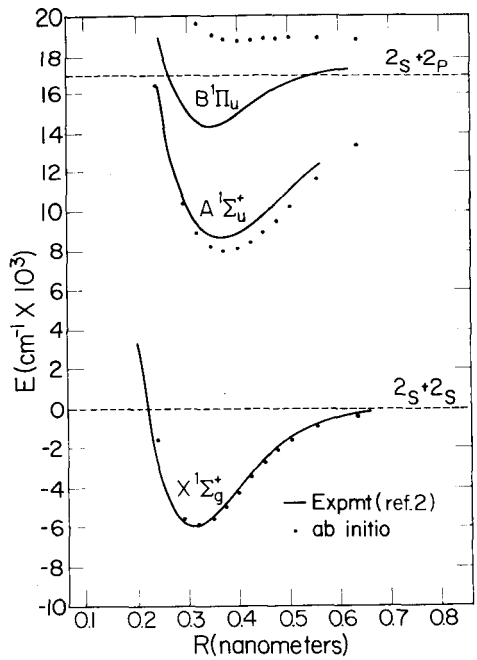

FIG. 1. Experimental and theoretical potential energy curves for the singlet states of Na_2. The energy of two ^2S Na atoms has been chosen as zero for the experimental and theoretical curves. The theoretical curves for the A and B states have been shifted to agree with the experimental atomic splittings asymptotically.

TABLE III. Calculated energies[a] for the singlet states of Na_2.

R[b] (bohr)	$X\,^1\Sigma_g^+$	$A\,^1\Sigma_u^+$	$B\,^1\Pi_u$
2.0	−322.71063	−322.59839	−322.57062
4.5	−323.72211	−323.63831	−323.60204
5.5	−323.74053	−323.66581	−323.62500
6.0	−323.74179	−323.67218	−323.62986
6.5	−323.74043	−323.67540	−323.63225
7.0	−323.73764	−323.67642	−323.63320
7.5	−323.73420	−323.67594	−323.63339
8.0	−323.73065	−323.67442	−323.63327
8.5	−323.72733	−323.67222	−323.63307
9.0	−323.72445	−323.66956	−323.63290
9.5	−323.72207	−323.66663	−323.63281
10.5	−323.71877	−323.66045	−323.63286
12.0	−323.71637	−323.65173	−323.63325
∞	−323.71490	−323.63573	−323.64211

[a]Energies in hartrees. 1 hartree = 219 474 cm^{-1}.
[b]1 bohr = 0.0529177 nm.

TABLE IV. Configuration mixing coefficients for the $A\,^1\Sigma_u^+$ state of Na_2.

Configuration \ R[a]	4.5	6.0	9.0	∞
[core] $4\sigma_g 5\sigma_u$	0.97782	0.98190	0.97956	0.70711
[core] $4\sigma_u 5\sigma_g$	−0.05760	−0.06405	−0.12032	−0.70711
[core] $2\pi_u 2\pi_g$	0.20084	0.17781	0.16091	0.0
[core] $1\delta_u 1\delta_g$	−0.01436	−0.01267	−0.00972	0.0

[a]Nuclear separation in bohrs. 1 bohr = 0.0529177 nm.

1 has been adjusted so that the calculated and experimental asymptotic energies agree. If the sum of the atomic energies was used as the theoretical asymptote, rather than the restricted-core calculated energy, the calculated potential well would be slightly more shallow than the experimental well. The long range behavior of the $A\,^1\Sigma_u^+$ potential energy curve is due to the attractive dipole–dipole resonance forces that occur for excited states of molecules composed of two identical atoms. King and Van Vleck[13] have shown that the interaction for an $SP+PS$ system in a $^1\Sigma_u^+$ state is

$$U(R) = -2\mu^2/R^3, \qquad \text{(II. 8)}$$

where μ is one of the Zeeman components of the atomic $S \rightarrow P$ dipole transition integral (e.g., $\langle 3s|z|3p_0\rangle$). For sodium $\mu^2 = 6.31$ a.u. [1 a.u. $= (2.54\ \text{D})^2$].

E. Results for the $B\,^1\Pi_u$ state

Although the $B^1\Pi_u$ state is not of primary concern here, it was computed for the purpose of comparing the theoretical $B \rightarrow X$ transition moment with the experimentally determined values of Hessel *et al.*[5] and Demtröder *et al.*[6] The principle $^1\Pi_u$ configuration at R_e is [core] $4\sigma_g 2\pi_u$. A second configuration [core] $4\sigma_u 2\pi_g$ was added to insure proper dissociation. Two more configurations $5\sigma_g 3\pi_u$ and $5\sigma_u 3\pi_g$ were also included in the final wavefunction. Due to computer program limitations two potentially important configurations [core] $2\pi_u 1\delta_g$ and [core] $2\pi_g 1\delta_u$ were not included in the wavefunction. Although these configurations may be energetically important, they are not connected to the principal ground state configurations by the dipole moment operator. Consequently, their major effect on the transition moment is through the renormalization of the $B^1\Pi_u$ CI mixing coefficients. This effect would amount only to a few percent even if the CI mixing coefficients of the missing configurations were as large as 0.2.

The potential energy curve for $B^1\Pi_u$ is tabulated in Table III and plotted in Fig. 1. The asymptote of the theoretical curve in Fig. 1 has been adjusted to agree with the experimental $^2S \rightarrow {}^2P$ excitation energy. At large R, dipole–dipole resonance forces cause the $^1\Pi_u$ curve to be repulsive[13] by the amount

$$U(R) = \mu^2/R^3. \qquad \text{(II. 9)}$$

The theoretical $^1\Pi_u$ curve is totally unbound, but does show a dip near the proper R_e value. Much of the energetic deficiency can be attributed to the missing configurations discussed above. It has been suggested,[14] however, that the state takes on considerable diffuse Rydberg character near R_e and the basis set used in our calculations does not contain sufficiently diffuse STO's to account for this phenomenon. We have not explored this problem in detail, but the excellent agreement of the $B \rightarrow X$ transition moment with experimentally determined values leads us to believe that the excluded configurations, rather than the basis set, is at fault.

TABLE V. Dipole transition moments[a] for Na_2.

R[b] (bohr)	$X\,^1\Sigma_g^+ \rightarrow A\,^1\Sigma_u^+$	$X\,^1\Sigma_g^+ \rightarrow B\,^1\Pi_u$
2.0	7.203	6.938
4.5	8.150	7.232
5.5	8.927	7.459
6.0	9.351	7.581
6.5	9.727	7.681
7.0	10.082	7.796
7.5	10.374	7.917
8.0	10.578	8.045
8.5	10.672	8.173
9.0	10.651	8.297
9.5	10.530	8.407
10.5	10.121	8.540
12.0	9.541	8.751
∞	8.938	8.994

[a]Transition moments in debyes. 1 D $= 10^{-18}$ esu cm.
[b]1 bohr $= 0.0529177$ nm.

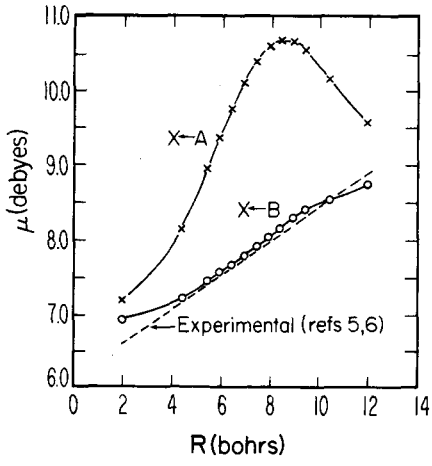

FIG. 2. Theoretical and experimental transition dipole moments of Na_2 as a function of nuclear separation. The solid lines are the theoretically determined values and the dashed line is the experimental curve for $B \rightarrow X$ from Refs. 5 and 6.

III. TRANSITION PROBABILITIES AND LIFETIMES

A. Dipole transition moments

The dipole transition operator for the $A\,^1\Sigma_u^+ \rightarrow X\,^1\Sigma_g^+$ transition is simply $\sum_i z_i$ in atomic units, where the sum runs over all electrons. Since the core electronic distributions are highly localized and change very little during the transition, the value of transition moment integral $\mu_{A\rightarrow X} = \langle {}^1\Sigma_u^+ | \sum z_i | {}^1\Sigma_g^+ \rangle$ is determined primarily by the two valence electrons. A tabulation of the transition moment is given in Table V and is plotted in Fig. 2. At R_e of the A state the value is about 10.2 D. A maximum of 10.7 D occurs at a distance of 8.5 bohr.

The value of $\mu^2_{A\rightarrow X}$ at $R=\infty$ can be determined analytically. Considering only the two valence electrons, the asymptotic form of the $X\,^1\Sigma_g^+$ wavefunction, in localized notation, is

$$\psi(X\,^1\Sigma_g^+) = 1/\sqrt{2}\,[3s_A(1)\,3s_B(2) + 3s_A(2)\,3s_B(1)]\Theta_{\text{spin}}, \qquad \text{(III. 1)}$$

where Θ_{spin} is the antisymmetric singlet spin function. For the $A\,^1\Sigma_u^+$ wavefunction, we have from Eq. (II. 6)

$$\psi(A\,^1\Sigma_u^+) = \tfrac{1}{2}[3s_A(1)\,3p\sigma_B(2) + 3p\sigma_A(1)\,3s_B(2) + 3s_A(2)\,3p\sigma_B(1) + 3p\sigma_A(2)\,3s_B(1)]\Theta_{\text{spin}}. \quad \text{(III. 2)}$$

Taking the matrix element of the operator $z_1 + z_2$ we get

$$|\langle A\,^1\Sigma_u^+|\, z_1 + z_2\,|X\,^1\Sigma_g^+\rangle|^2_{R=\infty} = 2\,|\langle 3p\sigma\,|\,z\,|\,3s\rangle|^2. \quad \text{(III. 3)}$$

The squared integral on the right is one Zeeman component of the atomic transition integral and is equal to 6.31 a.u.[15] The square of the molecular transition dipole matrix element at $R=\infty$ should be 12.62 a.u. Our calculated asymptotic value is 12.37 a.u.

The $B \rightarrow X$ transition moment, which is tabulated in Table V and plotted in Fig. 2, shows considerably less variation with R than $A \rightarrow X$. The theoretically computed curve is remarkably close to the experimental curve at all important R values. At $R=\infty$, the $B \rightarrow X$ transition moment is slightly different from the $A \rightarrow X$ value because the Π projection of the ^2P atomic wavefunction is slightly different from the Σ projection.

Tango and Zare[16] have calculated transition moments for the alkali dimers using valence wavefunctions constructed from undistorted Coulomb orbitals. The dependence of their computed transition moments on R is considerably different from the *ab initio* results reported here, which implies that their linear combination of atomic orbitals approach does not produce the correct molecular charge distributions. In addition, their results do not give the correct asymptotic limit because of an apparent misinterpretation of the asymptotic forms of the wavefunctions as discussed above.

B. Transition probabilities

The A value for a diatomic v, J transition is given by

$$A_{if} = \frac{64\pi^4\nu^3_{if}}{3h}\,\frac{S(J_i, J_f)}{(2J_i+1)}\,|\langle v_i J_i\,|\,\mu_{if}\,|\,v_f J_f\rangle|^2, \quad \text{(III. 4)}$$

TABLE VI. A values (in units of 10^4 sec^{-1}) for the $A\,^1\Sigma_u^+ \rightarrow X\,^1\Sigma_g^+$ transition in Na_2 with $J_i = 35$ and $J_f = 36$.

v_f \ v	0	1	2	3	4	5
0	3	21	68	153	269	394
1	29	132	303	464	520	438
2	117	366	533	445	196	18
3	300	572	405	76	19	195
4	545	516	69	66	288	235
5	743	217	48	320	175	0
6	791	5	314	200	5	207
7	671	114	350	0	230	165
8	459	408	100	184	205	5
9	256	590	13	328	1	215
10	116	537	252	124	167	161
11	43	349	509	7	297	2
12	13	171	525	241	85	210
13	3	63	351	501	27	249
14		18	165	494	312	23
15		4	56	303	525	107
16			14	125	435	433
17			2	36	220	519
18				7	73	330
19				1	15	126
20					2	29
21						4

TABLE VII. A values (in units of 10^4 sec^{-1}) for the $A\,^1\Sigma_u^+ \rightarrow X\,^1\Sigma_g^+$ transition in Na_2 with $J_i = 35$ and $J_f = 34$.

v_f \ v	0	1	2	3	4	5
0	3	20	64	145	256	378
1	27.	125	289	447	506	432
2	111	350	516	439	200	21
3	286	554	402	82	15	182
4	523	508	75	57	275	236
5	718	222	40	308	180	0
6	771	7	297	204	3	194
7	659	102	346	1	216	169
8	455	385	107	168	208	2
9	257	571	9	321	3	203
10	118	529	231	131	151	166
11	44	349	488	4	292	0
12	13	173	516	219	94	193
13	3	65	351	480	20	250
14		19	169	487	287	30
15		4	59	306	507	90
16			15	129	433	407
17			3	38	225	509
18				7	76	334
19					17	132
20					2	32
21						4

where ν_{if} is the transition energy in cm^{-1}, μ_{if} is the electronic transition moment, and $S(J_i, J_f)$ is the Hönl–London factor.[17] The subscripts i and f refer to the initial and finial states, respectively. In our calculations the transition frequencies were computed from the spectroscopic constants of Hessel and Kusch.[2] The molecular potentials for the A and X states were taken as the experimental RKR curves plus the rotational barrier

$$U(R) = U_{\text{RKR}}(R) + J(J+1)/R^2. \quad \text{(III. 5)}$$

The wavefunctions $<vJ|$ were obtained from a computer program written by Julienne[18] which solves the one-dimensional Schödinger equation using the method of Gordon.[19] The potentials and the transition moment μ were interpolated by cubic spline polynominals during the wavefunction generation and integration.

In Tables VI and VII we have tabulated the computed A values for the lowest six levels of the $A\,^1\Sigma_u^+$ state for $J_i = 35$, which is the maximum of the rotational distribution at 400 °K. The ordering of the A values for these low vibrational levels is not very sensitive to the rotational quantum number. The transitions with $\Delta J = (J_i - J_f) = +1$ are several percent stronger than those with $\Delta J = -1$. The strongest transition is $(v_i, v_f) = (0, 6)$ with an A value of 7.91×10^6 sec^{-1} for $\Delta J = +1$. The (0, 5) transition is only slightly less intense. These two transitions are also predicted to be the most intense by Frank–Condon factor (FCF) calculations. In all cases we find that the relative intensities of transitions from a single initial level to adjacent final vibrational levels are predicted correctly by FCF values. However, for transitions to widely spaced final levels, the variation of the dipole moment with internuclear distance becomes important and the actual relative intensities are considerably different from the FCF ratios. For example, the ratio of FCF's for transitions (2, 12) and

(2, 2) is 1.19, with (2, 12) having the largest FCF for all transitions from $v_i = 2$. From Table VI we see that the ratio of A values is (2, 12)/(2, 2) = 0.98, with (2, 2) being the most intense transition from $v_i = 2$. These large differences in relative intensity predictions could be easily verified experimentally.

Our calculations of the A values have not included interactions of the $A\,^1\Sigma_u^+$ state with other excited molecular states. However, Kusch and Hessel[3] have observed perturbations of some A-state levels due to a curve crossing with the $a\,^3\Pi_u$ state. These perturbations shift the energies of the A-state v, J levels by a small amount and also mix the singlet and triplet wavefunctions.[4] The singlet–triplet mixing is rather large near the curve crossing, and must reduce some of the A values. We have not explored these effects in detail.

C. Lifetimes

The radiative lifetimes for the v, J levels of the $A\,^1\Sigma_u^+$ state were computed by summing the calculated A values over final states

$$\frac{1}{\tau_i} = \sum_f A_{if}. \qquad \text{(III. 6)}$$

The lifetimes of the first 30 vibrational levels are given in Table VIII for J_i values of 20, 35, and 50. All significant A values were included in the sum. For $v_i = 15$, approximately 30 X-state levels were needed to converge the sum. For $v_i = 30$, it was necessary to sum over all ground state levels to achieve the correct lifetime. For levels higher than $v_i = 30$, transitions to the ground state continuum must be considered. The calculated lifetimes in Table VIII do not exhibit a strong J dependence. It is somewhat surprising to see a nearly constant lifetime for all vibrational levels even though the transition dipole moment exhibits a significant variation with internuclear distance.

Kleppner[7] has experimentally observed the lifetimes of several $A\,^1\Sigma_u^+$ vibrational levels by a molecular beam, laser-induced fluorescence technique. Individual rotation lines were not resolved. Our calculations for $J_i = 35$ are compared to the experimental values in Table IX. The agreement of theory and experiment is very good, even for the trend to slightly longer lifetimes for higher vibrational levels.

IV. CONCLUDING REMARKS

Ab initio calculations with carefully chosen basis sets, configurations, and convergence criteria can provide accurate values for molecular properties, including those, such as the transition dipole moment, which are very sensitive to wavefunction optimization. In the case of Na_2 we have produced transition dipole moment curves which give excellent agreement with experimentally determined transition moments ($B\,^1\Pi_u \rightarrow X\,^1\Sigma_g^+$) and lifetimes ($A\,^1\Sigma_u^+ \rightarrow X\,^1\Sigma_g^+$).

The Na_2 $A \rightarrow X$ transition exhibits lifetimes which are nearly independent of vibrational and rotational level at about 12.5 nsec. The strongest individual transition (for $J = 35$) is $v_i = 0$ to $v_f = 6$ with an A value 8×10^6 sec^{-1}.

TABLE VIII. Lifetimes (in nsec) of several v, J levels of $A\,^1\Sigma_u^+$ Na_2.

v	$J=20$	$J=35$	$J=50$
0	12.33	12.38	12.45
5	12.42	12.46	12.52
10	12.48	12.52	12.58
15	12.53	12.56	12.63
20	12.56	12.58	12.64
25	12.55	12.58	12.62
30	12.42	12.51	12.32

TABLE IX. Comparison of theoretical and experimental lifetimes for Na_2 $A\,^1\Sigma_u^+ \rightarrow X\,^1\Sigma_g^+$.

v	Experimental[a,b]	Theory ($J=35$)
1	12.2 ± 0.3	12.4
2	12.3 ± 0.4	12.4
6	12.3 ± 0.3	12.5
7	12.8 ± 0.5	12.5
21	12.9 ± 0.3	12.6
22	12.6 ± 0.2	12.6
24	13.0 ± 0.2	12.6
25	12.8 ± 0.2	12.6

[a]Reference 7.
[b]Lifetimes in nsec.

*Research supported in part by the United States Energy Research and Development Administration under contract number E(49-1)-3800, and in part by the Advanced Research Projects Agency under ARPA Order 891, Amendment #11.

[1]G. York and A. Gallagher, "High Power Gas Lasers Based on Alkali-Dimer A–X Band Radiation," Joint Institute for Laboratory Astrophysics Report No. 114, University of Colorado at Boulder, 1974 (unpublished).
[2]M. M. Hessel and P. Kusch (in preparation).
[3]P. Kusch and M. M. Hessel, J. Chem. Phys. 63, 4087 (1975).
[4]M. M. Hessel and P. Kusch, Abstracts MN8, Thirty-First Symposium on Molecular Spectroscopy, Ohio State University, Columbus, Ohio (June 1976).
[5]M. M. Hessel, E. W. Smith, and R. E. Drullinger, Phys. Rev. Lett. 33, 1251 (1974).
[6]W. Demtröder, W. Stetzenbach, M. Stock, and J. Witt, J. Mol. Spectrosc. 61, 382 (1976).
[7]T. W. Ducas, M. G. Littman, M. L. Zimmerman, and D. Kleppner, J. Chem. Phys. 65, 842 (1976).
[8]P. J. Bertoncini and A. C. Wahl (unpublished).
[9]G. Das and A. C. Wahl, "BISON-MC: A FORTRAN Computing System for Multiconfiguration Self-Consistent-Field Calculations on Atoms, Diatoms, and Polyatoms," Argonne National Laboratory Report No. ANL 7955 (1972).
[10]P. S. Bagus, T. L. Gilbert, and C. C. J. Roothaan, J. Chem. Phys. 56, 5195 (1972).
[11]N. Bardsley, D. Norcross, and R. Junker, Chem. Phys. Lett. 37, 502 (1976).
[12]P.-O. Löwdin and H. Shull, Phys. Rev. 101, 1730 (1956).
[13]G. W. King and J. H. Van Vleck, Phys. Rev. 55, 1165 (1939).
[14]N. Bardsley, S. V. O'Neil, and N. Winter (private communications).
[15]J. K. Link, J. Opt. Soc. Am. 56, 1195 (1966).
[16]W. J. Tango and R. N. Zare, J. Chem. Phys. 53, 3094 (1970).
[17]G. Herzberg, *Molecular Spectra and Molecular Structure* I. *Spectra of Diatomic Molecules* (Van Nostrand, Princeton, 1950), p. 208.
[18]P. Julienne (private communication).
[19]R. Gordon, J. Chem. Phys. 51, 14 (1969).